LETTER

doi:10.1038/nature09454

Clinical efficacy of a RAF inhibitor needs broad target blockade in *BRAF*-mutant melanoma

Gideon Bollag[1], Peter Hirth[1], James Tsai[1], Jiazhong Zhang[1], Prabha N. Ibrahim[1], Hanna Cho[1], Wayne Spevak[1], Chao Zhang[1], Ying Zhang[1], Gaston Habets[1], Elizabeth A. Burton[1], Bernice Wong[1], Garson Tsang[1], Brian L. West[1], Ben Powell[1], Rafe Shellooe[1], Adhirai Marimuthu[1], Hoa Nguyen[1], Kam Y. J. Zhang[1], Dean R. Artis[1], Joseph Schlessinger[2], Fei Su[3], Brian Higgins[3], Raman Iyer[3], Kurt D'Andrea[4], Astrid Koehler[3], Michael Stumm[3], Paul S. Lin[1], Richard J. Lee[3], Joseph Grippo[3], Igor Puzanov[5], Kevin B. Kim[6], Antoni Ribas[7], Grant A. McArthur[8], Jeffrey A. Sosman[5], Paul B. Chapman[9], Keith T. Flaherty[4]†, Xiaowei Xu[4], Katherine L. Nathanson[4] & Keith Nolop[1]

B-RAF is the most frequently mutated protein kinase in human cancers[1]. The finding that oncogenic mutations in *BRAF* are common in melanoma[2], followed by the demonstration that these tumours are dependent on the RAF/MEK/ERK pathway[3], offered hope that inhibition of B-RAF kinase activity could benefit melanoma patients. Herein, we describe the structure-guided discovery of PLX4032 (RG7204), a potent inhibitor of oncogenic B-RAF kinase activity. Preclinical experiments demonstrated that PLX4032 selectively blocked the RAF/MEK/ERK pathway in *BRAF* mutant cells and caused regression of *BRAF* mutant xenografts[4]. Toxicology studies confirmed a wide safety margin consistent with the high degree of selectivity, enabling Phase 1 clinical trials using a crystalline formulation of PLX4032 (ref. 5). In a subset of melanoma patients, pathway inhibition was monitored in paired biopsy specimens collected before treatment initiation and following two weeks of treatment. This analysis revealed substantial inhibition of ERK phosphorylation, yet clinical evaluation did not show tumour regressions. At higher drug exposures afforded by a new amorphous drug formulation[4,5], greater than 80% inhibition of ERK phosphorylation in the tumours of patients correlated with clinical response. Indeed, the Phase 1 clinical data revealed a remarkably high 81% response rate in metastatic melanoma patients treated at an oral dose of 960 mg twice daily[5]. These data demonstrate that *BRAF*-mutant melanomas are highly dependent on B-RAF kinase activity.

PLX4032 belongs to a family of mutant B-RAF kinase inhibitors discovered using a scaffold-based drug design approach[6]. The crystallography-guided approach allowed optimization of a compound with modest preference for the mutated form of B-RAF (B-RAF(V600E)) in comparison to wild-type B-RAF. Supplementary Table 1 summarizes the differential ability for PLX4032 to inhibit the activity of over 200 kinases. PLX4032 displays similar potency for B-RAF(V600E) (31 nM) and c-RAF-1 (48 nM) and selectivity against many other kinases, including wild-type B-RAF (100 nM). Whereas the vast majority of kinases are minimally affected, several were found that were also inhibited at $<$100 nM concentrations in biochemical assays; to date, inhibition of these non-RAF kinases such as ACK1 (also known as TNK2), KHS1 (also known as MAP4K5) and SRMS has not been tested in cellular assays. As previously demonstrated for the related B-RAF inhibitor PLX4720 (ref. 6), the biochemical selectivity of PLX4032 translates to cellular selectivity: potent inhibition of ERK phosphorylation and cell proliferation occurs exclusively in *BRAF*-mutant cell lines[4].

PLX4032 was co-crystallized with a protein construct that contained the kinase domain of B-RAF(V600E). PLX4032 (Fig. 1a) binds in the active site of one of the protomers in the non-crystallographic-symmetry related dimer (Fig. 1). As previously described for the related RAF inhibitor PLX4720 (PDB ID: 3C4C)[6], the PLX4032-bound protomer adopts the DFG-in conformation to enable the formation of a unique hydrogen bond between the backbone NH of Asp 594 and the sulfonamide nitrogen of PLX4032 (Fig. 1b). In addition, PLX4032-binding causes an outward shift in the regulatory αC helix, which may explain why the effect of PLX4720 and PLX4032 on RAF dimerization is in stark contrast to other RAF inhibitors such as AZD-628 and GDC-0879 (Fig. 1c)[7]. The apo-protomer displays the DFG-in conformation with the activation loop locked away from the ATP-binding site by a salt-bridge between Glu 600 and Lys 507 (Fig. 1d).

In *BRAF(V600E)*-mutant xenograft studies, PLX4032 demonstrated dose-dependent inhibition of tumour growth, with higher exposures resulting in tumour regression (Fig. 2a and ref. 4). Efficacy could be demonstrated in cell lines and xenografts bearing either homozygous or heterozygous *BRAF* mutations. By contrast, no effect was observed on melanoma xenograft growth if both *BRAF* alleles were wild-type[4,6]. Due to their consistent pharmacokinetics in rodents, PLX4032 and PLX4720 were prioritized over a panel of related compounds that all had similar activities *in vitro* and *in vivo*. For further drug development, PLX4032 was chosen (over PLX4720) because its pharmacokinetic properties scaled more favourably in beagle dogs and cynomolgus monkeys.

In order to estimate PLX4032 exposures (as defined by AUC_{0-24}, the area under the plasma concentration time curve over the dosing period of 24 h) that correlated with tumour response, conventionally formulated daily oral doses of PLX4032 were administered in the *BRAF(V600E)*-bearing colorectal cancer COLO205 xenograft model. In this model, tumour growth inhibition was modest at 6 mg kg^{-1} ($AUC_{0-24} \sim 50$ μM h), tumour stabilization was seen at 20 mg kg^{-1} once daily (QD) ($AUC_{0-24} \sim 200$ μM h), and significant tumour regressions were observed at 20 mg kg^{-1} twice daily (BID) ($AUC_{0-24} \sim 300$ μM h). *BRAF(V600E)*-bearing melanoma xenograft models, including NCI-LOX and COLO829 are also sensitive to PLX4032 (ref. 4).

Rats and beagle dogs were dosed for 28 days with increasing doses up to 1,000 mg kg^{-1} day^{-1}, and no toxicity was detected at any dose level. Likewise, no adverse effects were detected in a standard battery of safety pharmacology studies. Subsequent toxicology studies of longer duration, 26 weeks in rats and 13 weeks in dogs, further confirmed the tolerability of the compound. This safety profile was achieved in spite of very high compound exposures, reaching 2,600 μM h in rats and 820 μM h in dogs. The rat exposures exceeded those that were effective in patients (see below). Importantly, no histological changes were observed in the skin in any animal at any dose or duration of treatment, contrasting to results observed with other RAF inhibitors[7].

[1]Plexxikon Inc., 91 Bolivar Drive, Berkeley, California 94710, USA. [2]Yale University, 333 Cedar Street, New Haven, Connecticut 06520, USA. [3]Roche Pharmaceuticals, 340 Kingsland Street, Nutley, New Jersey 07110, USA. [4]Departments of Medicine and Pathology and Laboratory Medicine, Abramson Cancer Center, University of Pennsylvania, 421 Curie Boulevard, Philadelphia, Pennsylvania 19104, USA. [5]Vanderbilt University, 2220 Pierce Avenue, 777 PRB, Nashville, Tennessee 37232, USA. [6]The University of Texas M. D. Anderson Cancer Center, 1515 Holcombe Boulevard, Houston, Texas 77030, USA. [7]University of California, Los Angeles, 100 UCLA Medical Plaza, Los Angeles, California 90095, USA. [8]Peter MacCallum Cancer Centre, St Andrews Place, East Melbourne 3002, Australia. [9]Memorial Sloan Kettering Cancer Center, 1275 York Avenue, New York, New York 10065, USA. †Present address: Massachusetts General Hospital Cancer Center, Boston, MA 02114, USA.

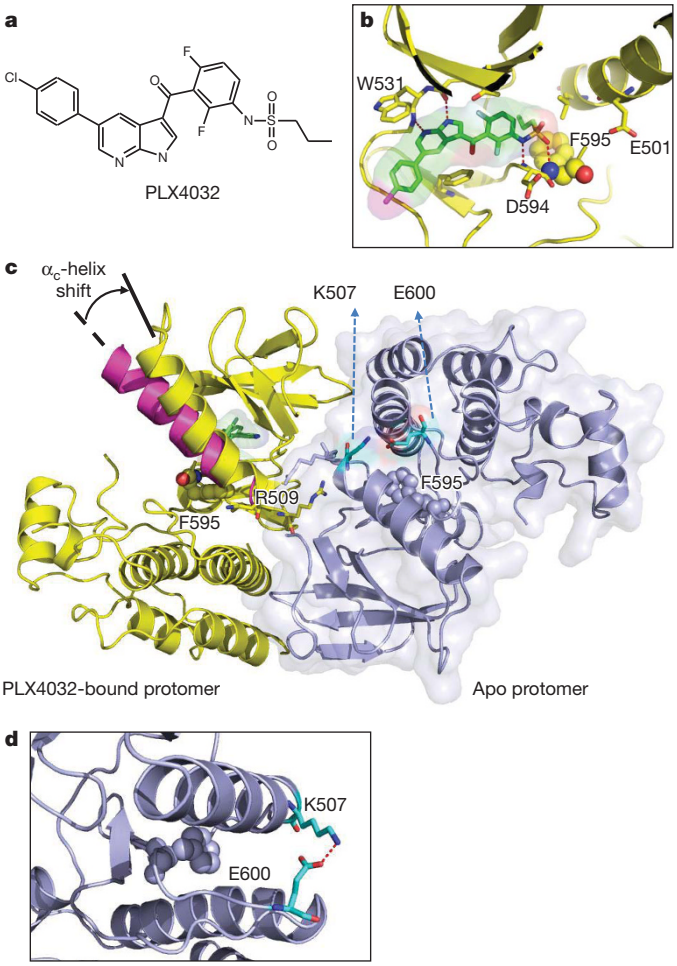

Figure 1 | Three-dimensional structure of PLX4032 binding to B-RAF(V600E). **a**, Chemical structure of PLX4032. **b**, Structure highlights the interactions of azaindole with the kinase hinge and the sulfonamide with the DFG loop, with F595 rendered in balls and other key protein residues shown as sticks. **c**, Structure of the asymmetric dimer of B-RAF(V600E) is shown with the PLX4032-protomer bound to PLX4032 coloured yellow (consistent with **b**). The surface outline of the other protomer (blue) is shown lightly shaded. Highlighted residues are R509 to reflect its role in anchoring the dimer and F595 to show that both protomers are in the DFG-in state. The α_c-helix shown in magenta is overlaid on the PLX4032-bound protomer to show its typical configuration in an unoccupied protomer; the binding of PLX4032 causes a shift of the α_c-helix as noted by the arrow. **d**, Magnified view of the salt bridge between Lys 507 and Glu 600 that helps prevent compound binding to the apo protomer.

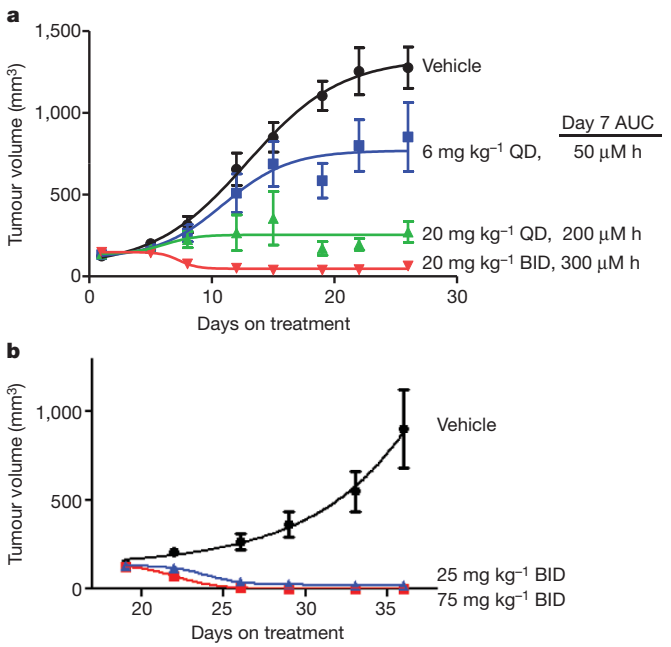

Figure 2 | Effect of PLX4032 on COLO205 xenograft tumour growth. Tumour volume measurements of mice treated by oral gavage with the indicated doses of PLX4032 or vehicle ($n = 10$ for all groups, error bars indicate standard error) are shown. **a**, Administration in conventional formulation occurred daily. Exposures measured on day 7 are shown. At the 6, 20 and 20 BID doses, 1/10, 1/10 and 8/10 animals achieved CR, respectively. **b**, Administration in the MBP formulation occurred twice daily. At the 25 mg kg^{-1} BID dose (blue), 7/10 animals achieved CR and 3/10 animals achieved PR; at the 75 mg kg^{-1} BID dose (red), all animals achieved CR.

PLX4032's performance in these preclinical toxicology studies provided the necessary safety data to support initiation of Phase 1 clinical testing in cancer patients. Clinical and pharmacokinetic results from this Phase 1 study have been reported recently[5]. In the initial stage of the Phase 1 study, cohorts of patients with advanced solid tumours were treated with escalating doses of PLX4032 (ranging from 200 to 1,600 mg), administered twice-daily (BID) as oral capsules. The initial crystalline formulation yielded modest drug exposures, so PLX4032 was reformulated as a micro-precipitated bulk powder (MBP), and doses ranging from 160 to 1,120 mg BID were sequentially evaluated. Preclinical experiments in mice (Fig. 2b and ref. 4) and dogs demonstrated that the MBP formulation substantially increased drug bioavailability, an approximately tenfold improvement. This improved bioavailability was also observed in patients, with mean exposures at a 160 mg BID dose of the MBP formulation (day 15 $AUC_{0-24} = 185$ μM h) similar to a 1,600 mg BID dose of the original formulation (day 15 $AUC_{0-24} = 203$ μM h).

During the dose-escalation stage of the Phase 1 trial, 21 patients with metastatic melanoma, 16 with and 5 without *BRAF*-mutations, were treated at doses that achieved $AUC_{0-24} > 300$ μM h (ref. 5). Tumour dimensions were measured by computed tomography (CT). Ten patients with *BRAF*-mutant melanoma achieved tumour regressions qualifying as partial responses (PR, by response evaluation criteria in solid tumours (RECIST 1.0), >30% reduction in tumour dimensions) and one patient had a complete response (CR); none of the patients with melanomas lacking *BRAF* mutations achieved PR. These data along with preclinical evidence of selectivity for *BRAF*-mutant cell lines strongly justified limiting all further enrolment to patients with *BRAF*-mutant tumours. Dose-limiting toxicities detected at the 1,120 mg BID dose included fatigue, rash and joint pain[5]. Therefore, 960-mg BID was identified as the maximum tolerated dose (MTD), and subsequently a cohort of 32 patients with *BRAF*-mutant melanoma was enrolled at the MTD in an extension of the Phase 1 study.

At the 960-mg BID dose, the steady state PLX4032 concentration was 86 μM and the AUC_{0-24} was 1,741 μM h; the half-life was estimated to be 50 h (ref. 5). Out of the 32 patients treated at this dose, 24 experienced tumour regressions qualifying as PRs and two patients had CRs. *BRAF(V600E)* mutation status was assessed by a real-time polymerase chain reaction (PCR) assay as described in Methods[5,8], and many of the samples were sequenced for verification of the PCR result. The reliability of the PCR assay is currently being assessed in concurrent Phase 2 and Phase 3 trials. The *BRAF(V600E)* allele was detected by the PCR assay in 46 of the 48 *BRAF*-positive patients described above. Interestingly, subsequent sequencing revealed that tumours from the two patients lacking the *BRAF(V600E)* mutation were found to carry the *BRAF(V600K)* mutation and were among the better responders (71% and 100% reduction in tumour dimensions); an additional *BRAF(V600K)* response has been recently published[9].

During the dose escalation stage of the study, a cohort of patients had paired tumour biopsies to evaluate pathway inhibition, the first taken

before initiation of PLX4032 treatment and the second taken after 14 days of PLX4032 treatment. This paired-biopsy cohort of patients captured a wide inter-patient range of steady state PLX4032 exposures. In addition to expected inter-patient variability in drug clearance, these patients were treated at different doses and with the two different formulations (one crystalline and one amorphous). To monitor ERK pathway activity, phosphorylated-ERK (pERK) levels were determined by immunohistochemistry (IHC), both in the nucleus and in the cytoplasm. To monitor proliferation, Ki67 levels also were measured.

As shown in Supplementary Table 2, levels of pERK and Ki67 were decreased in most biopsies following 2 weeks of dosing with PLX4032, even in patients with modest drug exposure. Patients exposed to plasma levels of PLX4032 less than 300 μM h experienced no measurable decreases in tumour burden. In contrast, patients exposed to higher plasma levels of PLX4032 experienced tumour regression, often achieving PRs as defined by RECIST criteria (Supplementary Table 2). Representative pictures illustrating decreases in ERK phosphorylation and Ki67 are shown in Fig. 3a and b. Interestingly, decreases in cytoplasmic pERK correlated well with tumour response (Fig. 3c), whereas changes in nuclear pERK correlated poorly (Fig. 3d). In general, nuclear pERK was more sensitive to compound levels than cytoplasmic pERK, consistent with the idea that nuclear ERK responds very quickly to phosphorylation/dephosphorylation events, whereas cytoplasmic ERK phospho-events are buffered by the many cytoplasmic scaffolding proteins. As further evidenced in Supplementary Table 2, the improved pathway inhibition and tumour responses correlate with higher plasma drug exposures. In patients with tumour regressions, pathway analysis typically showed greater than 80% inhibition of cytoplasmic ERK phosphorylation (Fig. 3c). This result indicates that near-complete inhibition of ERK signalling may be needed for significant tumour response.

A growing body of literature shows that oncogenic BRAF is an important stimulator of metabolic activity[10,11], and in preclinical studies PLX4032 rapidly inhibits fluoro-deoxy-glucose (FDG) uptake specifically in BRAF(V600E) mutant melanoma cell lines[12]. Therefore, FDG uptake in patients on the PLX4032 trial was assessed using positron emission tomography (PET) imaging before treatment and following 2 weeks of dosing. All of the assessable patients treated with MBP-formulated PLX4032 experienced major reductions in FDG uptake. Representative FDG-PET images are shown in Fig. 4.

Toxicities such as fatigue, rash and joint pain in the treated patients are detailed separately[5]. Thirty-one percent of the patients treated at the MTD developed skin lesions described as cutaneous squamous cell carcinomas, keratoacanthoma type[5]. This apparent drug-induced effect is of particular interest, because investigators studying three other RAF inhibitors, sorafenib[13–15], XL281 (ref. 16) and GSK2118436 (ref. 17) also have noted these skin lesions in a subset of treated patients. Although the occurrence of these treatment-emergent tumours warrants careful dermatological monitoring of patients during PLX4032 treatment, it should be noted that these lesions were resected, and no patients discontinued PLX4032 due to this drug-induced effect[5]. These skin lesions generally appear within a few months of treatment initiation in sun-exposed areas of skin, suggesting that pre-existing oncogenic mutations may potentiate the RAF inhibitor effects.

Recent publications suggest a potential mechanism that may in part account for the keratinocyte proliferation noted in some patients on study[7,18,19]. These reports follow up on prior descriptions of paradoxical activation of the RAF/MEK/ERK pathway by RAF kinase inhibitors[20–22]. Current evidence suggests that wild-type RAF kinase activity can be activated by RAF dimerization[23]. RAF dimerization can be induced by RAF inhibitors: binding to one protomer—while inhibiting the kinase activity of that protomer—concurrently induces a conformational switch in the partner protomer via an undefined allosteric mechanism to activate RAF kinase activity[7,19]. This paradoxical activation occurs in cells in which RAS is activated either by mutation or by some other priming event. Modulation of RAF dimerization may not be the only unexpected effect of RAF inhibitors, because multiple additional factors

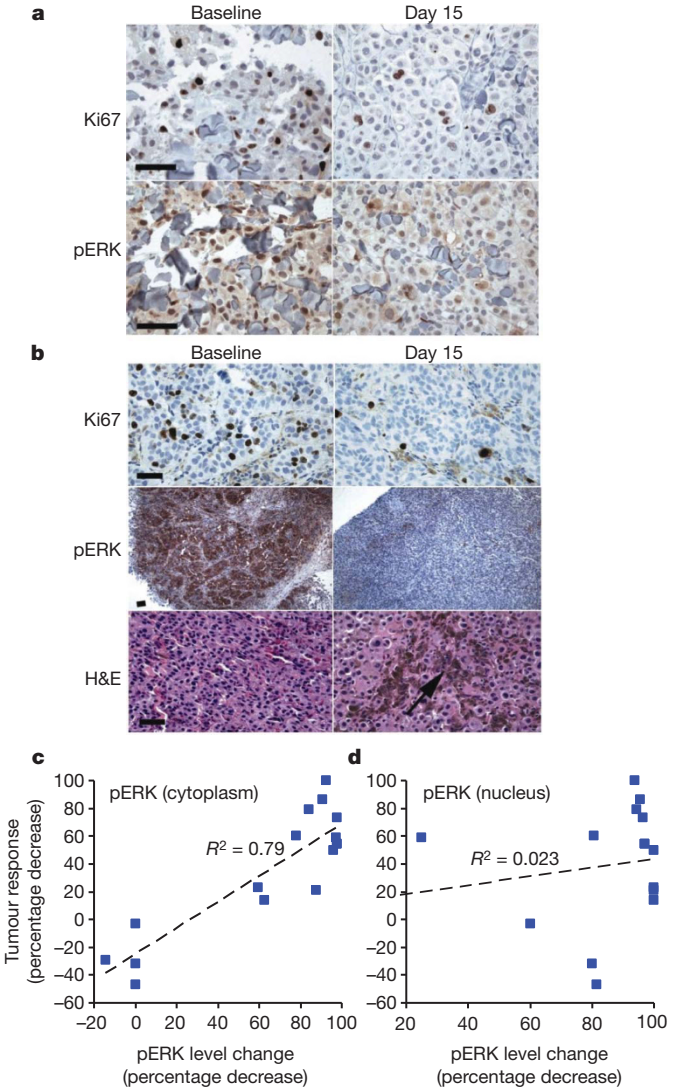

Figure 3 | Semi-quantitative immunohistochemistry (IHC) in paired tumour biopsies. Matched baseline and day 15 tumour samples are at the same magnification; the scale bar is 70 μm. **a**, Representative IHC for Ki67 and pERK staining is shown for patient 12. **b**, Representative IHC for Ki67, pERK and H&E (haematoxylin and eosin) staining is shown for patient 42. The arrow indicates tumour breakdown with macrophages engulfing the released melanin in the day 15 sample. **c**, Summary graph showing correlation of reduction in cytoplasmic pERK with tumour responses (data from Supplementary Table 2). **d**, Summary graph indicating weak correlation of reduction in nuclear pERK with tumour responses.

are involved in both positive (for example, KSR, SRC, CNK (also known as CNKSR)) and negative (for example, ERK), 14-3-3 (also known as YWHAQ), DUSP, RKIP (also known as PEBP1), RASSF) regulation of the RAF/MEK/ERK signalling pathway[24,25].

The ability of PLX4032 to cause tumour regression in a large proportion of patients with *BRAF*-mutant, advanced-stage, metastatic melanoma provides strong support for the hypothesis that the oncogenic B-RAF protein is a dominant driver of tumour growth and maintenance. These results are particularly interesting in that the *BRAF* mutation is likely an initiating event in melanoma tumorigenesis: the vast majority of benign nevi harbour the same *BRAF(V600E)* mutation[26]. Our current understanding of melanocyte biology suggests that the nevi are benign because the *BRAF* mutation alone (without cooperating mutations) induces senescence[27]. Clinical evaluation of sporadic nevi in patients treated at therapeutic doses revealed no effect of PLX4032 on nevi progression or regression. Additional descriptions

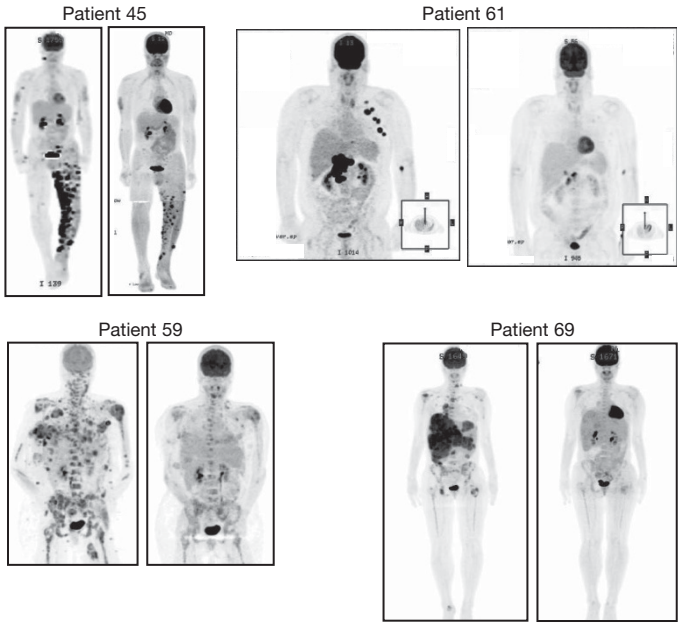

Figure 4 | Representative PET scans for patients taken pre-dose and following 2 weeks of dosing with PLX4032. Each of these image pairs demonstrates significant reduction in FDG uptake following PLX4032 treatment. Note that tumour regressions were later documented for each of these patients: best responses were 70% for patient 45, 70% for patient 59, 68% for patient 61 and 37% for patient 69.

of PLX4032 kinase selectivity, PLX4032 structure, and clinical pharmacokinetics and efficacy are included in Supplementary Information.

The durability of response to PLX4032 is still under evaluation. Median progression-free survival (PFS) in the Phase 1 extension cohort has not been reached but is currently estimated to be at least 7 months[5]. Although this compares rather favourably with a PFS of less than 2 months in historical analysis of large numbers of advanced melanoma patients[28], tumour re-growth occurs in many of the patients and the mechanisms of resistance are currently under investigation. Therefore, improved durability of response will be an important goal of further clinical trials. One potential strategy to meet this goal is to combine PLX4032 with other targeted agents, immunotherapy or chemotherapy. With a promising safety and efficacy profile, PLX4032 has the potential to anchor such combination treatments, and may thereby offer further improved treatment options for *BRAF*-mutant melanoma patients.

METHODS SUMMARY

PLX4032 was synthesized using the general procedures described previously[6]. Expression and purification of B-RAF, structure determination, protein kinase activity measurements and xenograft studies were carried out as described previously[6]. Clinical methods have also been described recently[5]. Melanoma patients were selected for study using previously described TaqMan methodology[8]. Semi-quantitative immunohistochemistry for pERK and Ki67 was performed on 5-μm-thick formalin-fixed paraffin-embedded tumour biopsies following haematoxylin and eosin staining to determine pathologic diagnosis and tissue morphology and integrity. The degree of phospho-ERK staining in the nucleus and cytoplasm was interpreted semi-quantitatively by assessing the intensity and extent of staining on the slides. For Ki67 staining, the percentage of positive cells was determined.

Received 19 May; accepted 31 August 2010.
Published online 7 September 2010.

1. Greenman, C. *et al.* Patterns of somatic mutation in human cancer genomes. *Nature* **446,** 153–158 (2007).
2. Davies, H. *et al.* Mutations of the *BRAF* gene in human cancer. *Nature* **417,** 949–954 (2002).
3. Solit, D. B. *et al.* BRAF mutation predicts sensitivity to MEK inhibition. *Nature* **439,** 358–362 (2006).
4. Yang, H. *et al.* RG7204 (PLX4032), a selective $BRAF^{V600E}$ inhibitor, displays potent antitumor activity in preclinical melanoma models. *Cancer Res.* **70,** 5518–5527 (2010).
5. Flaherty, K. *et al.* Inhibition of mutated, activated BRAF in metastatic melanoma. *N. Engl. J. Med.* **363,** 809–819 (2010).
6. Tsai, J. *et al.* Discovery of a selective inhibitor of oncogenic B-Raf kinase with potent antimelanoma activity. *Proc. Natl Acad. Sci. USA* **105,** 3041–3046 (2008).
7. Hatzivassiliou, G. *et al.* RAF inhibitors prime wild-type RAF to activate the MAPK pathway and enhance growth. *Nature* **464,** 431–435 (2010).
8. Koch, W. H. Technology platforms for pharmacogenomic diagnostic assays. *Nature Rev. Drug Discov.* **3,** 749–761 (2004).
9. Rubinstein, J. C. *et al.* Incidence of the V600K mutation among melanoma patients with BRAF mutations, and potential therapeutic response to the specific BRAF inhibitor PLX4032. *J. Transl. Med.* **8,** 67 (2010).
10. Esteve-Puig, R., Canals, F., Colome, N., Merlino, G. & Recio, J. A. Uncoupling of the LKB1-AMPKα energy sensor pathway by growth factors and oncogenic $BRAF^{V600E}$. *PLoS ONE* **4,** e4771 (2009).
11. Zheng, B. *et al.* Oncogenic B-RAF negatively regulates the tumor suppressor LKB1 to promote melanoma cell proliferation. *Mol. Cell* **33,** 237–247 (2009).
12. Søndergaard, J. N. *et al.* Differential sensitivity of melanoma cell lines with $BRAF^{V600E}$ mutation to the specific B-Raf inhibitor PLX4032. *J. Transl. Med.* **8,** 39 (2010).
13. Arnault, J. P. *et al.* Keratoacanthomas and squamous cell carcinomas in patients receiving sorafenib. *J. Clin. Oncol.* **27,** e59–e61 (2009).
14. Dubauskas, Z. *et al.* Cutaneous squamous cell carcinoma and inflammation of actinic keratoses associated with sorafenib. *Clin. Genitourin. Cancer* **7,** 20–23 (2009).
15. Kong, H. H. *et al.* Keratoacanthomas associated with sorafenib therapy. *J. Am. Acad. Dermatol.* **56,** 171–172 (2007).
16. Schwartz, G. K. *et al.* A phase I study of XL281, a selective oral RAF kinase inhibitor, in patients (Pts) with advanced solid tumors. *J. Clin. Oncol.* **27,** 3513 (suppl.), (2009).
17. Kefford, R. *et al.* Phase I/II study of GSK2118436, a selective inhibitor of oncogenic mutant BRAF kinase, in patients with metastatic melanoma and other solid tumors. *J. Clin. Oncol.* **28,** 8503 (suppl.), (2010).
18. Heidorn, S. J. *et al.* Kinase-dead BRAF and oncogenic RAS cooperate to drive tumor progression through CRAF. *Cell* **140,** 209–221 (2010).
19. Poulikakos, P. I., Zhang, C., Bollag, G., Shokat, K. M. & Rosen, N. RAF inhibitors transactivate RAF dimers and ERK signalling in cells with wild-type BRAF. *Nature* **464,** 427–430 (2010).
20. Courtois-Cox, S. *et al.* A negative feedback signaling network underlies oncogene-induced senescence. *Cancer Cell* **10,** 459–472 (2006).
21. Dougherty, M. K. *et al.* Regulation of Raf-1 by direct feedback phosphorylation. *Mol. Cell* **17,** 215–224 (2005).
22. Hall-Jackson, C. A. *et al.* Paradoxical activation of Raf by a novel Raf inhibitor. *Chem. Biol.* **6,** 559–568 (1999).
23. Rajakulendran, T., Sahmi, M., Lefrancois, M., Sicheri, F. & Therrien, M. A dimerization-dependent mechanism drives RAF catalytic activation. *Nature* **461,** 542–545 (2009).
24. Pratilas, C. A. *et al.* ^{V600E}BRAF is associated with disabled feedback inhibition of RAF-MEK signaling and elevated transcriptional output of the pathway. *Proc. Natl Acad. Sci. USA* **106,** 4519–4524 (2009).
25. Kolch, W. Coordinating ERK/MAPK signalling through scaffolds and inhibitors. *Nature Rev. Mol. Cell Biol.* **6,** 827–837 (2005).
26. Pollock, P. M. *et al.* High frequency of BRAF mutations in nevi. *Nature Genet.* **33,** 19–20 (2003).
27. Michaloglou, C. *et al.* $BRAF^{E600}$-associated senescence-like cell cycle arrest of human naevi. *Nature* **436,** 720–724 (2005).
28. Korn, E. L. *et al.* Meta-analysis of phase II cooperative group trials in metastatic stage IV melanoma to determine progression-free and overall survival benchmarks for future phase II trials. *J. Clin. Oncol.* **26,** 527–534 (2008).

Supplementary Information is linked to the online version of the paper at www.nature.com/nature.

Acknowledgements We thank L. Andries and M. Knaapen from HistoGeneX for evaluating paired biopsies, and also our colleagues at the Molecular Imaging Research division of Charles River Labs for conducting the xenograft studies. We also thank D. Heimbrook, S. Cheng, L. Burdette and B. Lestini for helpful comments on the manuscript. This research was funded in part by NIH grants to K.L.N. G.A.M. is supported by a Weary Dunlop Fellowship of the Cancer Council of Victoria.

Author Contributions G.B., P.H., C.Z., K.L.N. and K.N. designed studies, interpreted data and wrote the manuscript. J.T., G.H., E.A.B., B.W., G.T., B.L.W., B.P., R.S., A.M., H.N., F.S., and B.H. conducted or managed biochemical or biological studies. J.Z., P.N.I., H.C., W.S., D.R.A. and R.I. designed and conducted chemistry and formulation experiments. Y.Z. and K.Y.J.Z. conducted and interpreted structural studies. J.S. helped interpret data and write the manuscript. K.D., A.K., M.S. and X.X. designed, managed and interpreted biomarker studies. P.S.L., R.J.L., J.G., I.P., K.B.K., A.R., G.A.M., J.A.S., P.B.C. and K.T.F. managed or conducted clinical and translational studies.

Author Information Atomic and structural data have been deposited in Protein Data Bank under accession number 3OG7. Reprints and permissions information is available at www.nature.com/reprints. Readers are welcome to comment on the online version of this article at www.nature.com/nature. The authors declare competing financial interests: details accompany the full-text HTML version of the paper at www.nature.com/nature. Correspondence and requests for materials should be addressed to G.B. (gbollag@plexxikon.com).